

Removal of Fluoride using Quaternized Palm Kernel Shell as Adsorbents: Equilibrium Isotherms and Kinetics Studies

Ayu Haslija Bt Abu Bakar,^{a,f,*} Yin Shin Koay,^e Yern Chee Ching,^g
Luqman Chuah Abdullah,^{a,b} Thomas S. Y. Choong,^{a,b} Ma'an Alkhatib,^c
Mohsen Nourouzi Mobarekeh,^d and Nur Amirah Mohd Zahri^a

Palm kernel shell (PKS) core fibers, an agricultural waste, were chemically modified using N-(3-chloro-2-hydroxypropyl) trimethylammonium chloride (CHMAC) as a quaternizing agent. The potential of quaternized palm kernel shell (QPKS) as an adsorbent for fluoride in an aqueous solution was then studied. The quaternized palm kernel shell (QPKS) core fibers were characterized using Fourier transform infrared spectroscopy (FTIR) and a scanning electron microscope (SEM). The effect of various factors on the fluoride sequestration was also investigated. The results showed that with an increase in the adsorbent amount and contact time, the efficiency of fluoride removal was improved. The maximum fluoride uptake was obtained at pH 3 and a contact time of 4 h. The adsorption behavior was further investigated using equilibrium isotherms and kinetics studies. The results from these studies fit well into Freundlich, Redlich-Peterson, and Sips isotherm's with a coefficient of determination (R^2) of 0.9716. The maximum fluoride removal was 63%. For kinetics studies, the pseudo-second order was the best fit for fluoride, with an R^2 of 0.999. These results suggest that QPKS has the potential to serve as a low-cost adsorbent for fluoride removal from aqueous solutions.

Keywords: Fluoride removal; Quaternized palm kernel shells; Adsorption; Isotherms; Kinetics

Contact information: a: Department of Chemical and Environmental Engineering, Faculty of Engineering, Universiti Putra Malaysia, 43400 UPM Serdang, Selangor, D.E, Malaysia; b: Institute of Tropical Forestry and Forest Products (INTROP), Universiti Putra Malaysia, 43400 UPM Serdang, Selangor, D.E, Malaysia; c: Biotechnology Engineering Department, Kulliyah of Engineering, International Islamic University Malaysia (IIUM), Jalan Gombak, 53100, Malaysia; d: Department of Environment, Islamic Azad University, Khorasgan branch, Isfahan, Iran; e: Department of Bioproduct Research and Innovation, Institute of Bioproduct Development (IBD), Universiti Teknologi Malaysia, 81310 UTM Johor Bahru, Johor, Malaysia; f: Department of Chemical and Petroleum Engineering, Faculty of Engineering, Technology & Built Environment, UCSI University, 56000 Cheras, Kuala Lumpur, Malaysia; g: Department of Mechanical Engineering, University of Malaya, 50603 Kuala Lumpur, Malaysia;

* Corresponding author: chik_ija@yahoo.com, ayuhaslija@ucsiuniversity.edu.my

INTRODUCTION

Fluoride, a salt of the element fluorine, occurs primarily as sellaite (MgF_2), fluor spar (CaF_2), cryolite (Na_3AlF_6), and fluorapatite [$3\text{Ca}_3(\text{PO}_4)_2 \text{Ca}(\text{F},\text{Cl}_2)$]. It is an essential constituent for both humans and animals, depending on the total amount ingested or its concentration in drinking water. The presence of fluorine in drinking water, within permissible limits of 0.5 to 1.0 mg/L, is beneficial for the production and maintenance of healthy bones and teeth, while excessive intake of fluoride causes dental or skeletal fluorosis, which is a chronic disease that manifests through the mottling of teeth in mild

cases, and even the softening of bones and neurological damage in severe cases (Lounici *et al.* 1997; Srimurali *et al.* 1998; Hichour *et al.* 1999; Wang and Reardon 2001). The difference between desirable doses and toxic doses of fluoride is poorly defined, and fluoride may therefore be considered an essential mineral with a narrow margin of safety (WHO 1984). Table 1 shows the effect of prolonged exposure at high fluoride concentrations as dental fluorosis progresses to skeletal fluorosis (Dissanayake 1991).

Table 1. Effects of Prolonged Use of Drinking Water on Human Health Related to Fluoride Content (Dissanayake 1991)

F ⁻¹ concentration, (mg/L)	Health outcome
<0.5	Dental caries
0.5 to 1.5	Optimum dental health
1.5 to 4.0	Dental fluorosis
4.0 to 10	Dental and skeletal fluorosis
>10.0	Crippling fluorosis

High fluoride level wastewater is produced every day by industries using hydrofluoric acid as a cleaning agent, such as the semiconductor, solar cell, and metal manufacturing industries, or as a reactant or catalyst in the plastics, pharmaceutical, petroleum refining, and refrigeration industries. Untreated high-fluoride level wastewater is one of the key contributors to ground water and surface water pollution (Gupta and Suhas 2009; Malakootian *et al.* 2011). Thus, the problems associated with excess fluoride in water bodies can be highly endemic and widespread in many countries.

Fluoride removal technology has been a subject of interest among researchers for many years. Table 2 shows a comparison between various fluoride wastewater treatment methods (Bhatnagar *et al.* 2011).

Table 2. A Summary of Methods for Fluoride Treatment (Bhatnagar *et al.* 2011)

Methods	Advantages	Disadvantages
Ion exchange	No loss of sorbent	High operational
Reverse osmosis	Simple and low cost	Generation of toxic sludge
Electrodialysis	Effective	Complicated procedure
Electrochemical	Effective	High cost factor
Precipitation and coagulation	Effective	Generation of toxic sludge
Membrane process	No additives	Expensive installation
Nalgonda technique	Simple	High residual of aluminum

Most treatment methods impose high costs either in installing or maintaining the system. Even though some methods like reverse osmosis are simple and have low operating costs, there is still some secondary pollution generated. As such, the process used to dispose of the secondary pollution will also be costly. In contrast, the adsorption method has been reported as one of the most effective, economical, and environmentally friendly of the various defluoridation techniques (Kagne *et al.* 2008; Deng *et al.* 2011; Srivastav *et al.* 2013). The advantage of adsorption is its simplicity in design and operation. However, the selection of adsorbents also plays an important role in the adsorption process.

Malaysia accounts for 39% of the world's palm oil production and is the world's second biggest palm oil exporter, after Indonesia. Malaysia planted a total area of 5.03 million hectares of oil palms in June 2012 (MPOB 2012a), and produced 17 million tons of palm oil from January 2012 to November 2012 (MPOB 2012b). The process of crude palm oil extraction from fresh fruit bunches produces few types of agricultural waste, namely empty fruit bunch (EFB), palm kernel shell (PKS), fiber, and palm oil mill effluent (POME). The estimated percentage of palm oil mill waste produced is 14.6% of EFB, 10.4% PKS, 15.4% of fiber, and 6.3% POME on the basis of dry weight of fresh fruit bunch (FFB) (Yusoff 2006). Ng *et al.* (2012) reported that in the year 2010, Malaysia produced a total of 86.90 million tons of palm oil biomass and 5.2 million tons of palm kernel shell (PKS). PKS is a more suitable adsorbent material than other palm oil waste because of its high mechanical strength, porous surface, chemical stability, variable surface functional groups, and insolubility in water. Figure 1 shows images of palm kernel shell. The proximate chemical composition and elemental analysis for PKS are shown in Table 3, as reported by Idris *et al.* (2012) and Kim *et al.* (2010).



Fig. 1. Images of palm kernel shells

Table 3. Characteristics of PKS (Kim *et al.* 2010; Idris *et al.* 2012)

Proximate analysis ^a (wt.%)		
	Kim <i>et al.</i> 2010	Idris <i>et al.</i> 2012
Volatile matter	82.5	73.77
Fixed carbon	1.4	15.15
Ash	6.7	11.08
Moisture	9.4	-
Elemental analysis ^b (wt.%)		
Carbon	44.56	48.68
Hydrogen	5.22	4.77
Nitrogen	0.4	1.17
Sulfur	0.05	0.202
Oxygen	49.77	45.27
Chemical composition ^b (wt.%)		
Cellulose	33.04	-
Hemicellulose	23.82	-
Lignin	45.59	-
Extractives	9.89	-

^a Wet basis for Kim *et al.* (2010) and dry basis for Idris *et al.* (2012); ^b Ash-free basis

Quaternization is a surface chemical treatment that adds $R-NR'_3^+$ groups (where R represents cellulose, hemicellulose, or lignin structures and R' represents an alkyl group) onto the surface of lignocellulosic fibers *via* epoxy substitution to increase its affinity toward anionic substances by promoting ion-exchange adsorption (Malakootian *et al.* 2011; Bhatnagar *et al.* 2011). Cellulose is a straight-chain natural polymer that consists of a β -D-glucopyranose monomer and is covalently linked by a β -1,4-glycosidic bond. A molecule of cellulose has many hydroxyl groups attached, but reactions only happen to the hydroxyl group at C-6 conformations as a result of steric hindrance (Perez and Samain 2010). There are many quaternizing agents that can be used, depending on the reaction mechanism desired. The quaternizing agents most used in research are trimethylamine and N-(3-chloro-2-hydroxypropyl) trimethylammonium chloride (CHMAC). Quaternizing reactions using triethylamine as the quaternizing agent require pyridine as a catalyst and N,N-dimethylformamide (DMF) as a solvent, both of which are carcinogenic and expensive. Therefore, CHMAC is a preferred quaternizing agent, as only sodium hydroxide is needed in the reaction, which is a relatively cheap and safe chemical to use (Marshall and Wartelle 2004; de Lima *et al.* 2012). There are three reaction steps in a quaternization reaction; the interaction between cellulose and sodium hydroxide, epoxy formation from CHMAC, and the reaction between epoxide and the hydroxyl group of cellulose to produce ether, as shown in Fig. 2 (de Lima *et al.* 2012).

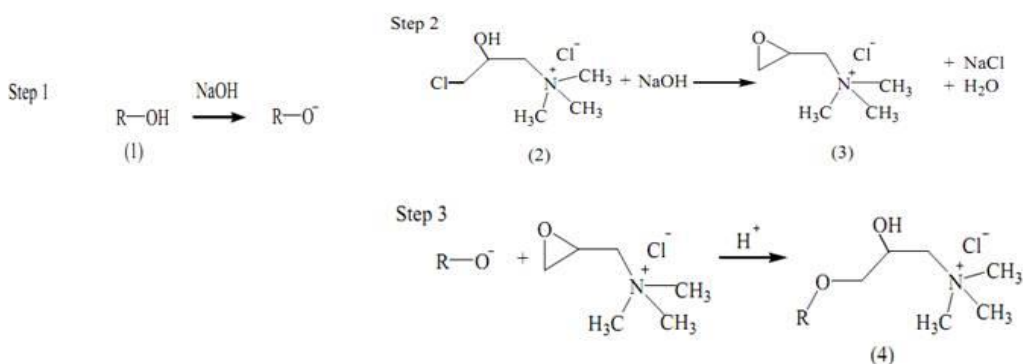


Fig. 2. Lignocellulose quaternization reaction scheme: (1) cellulose, (2) N-(3-chloro-2-hydroxypropyl), (3) trimethylammonium chloride epoxide, and (4) quaternized cellulose (de Lima *et al.* 2012)

Quaternized lignocellulosic fiber shows an increase in adsorption capacity and affinity toward anionic substrates as the quaternization treatment increases the porosity, surface area, and chelating functional groups. A summary of research conducted using quaternized lignocellulosic fiber as an adsorbent in the removal of anionic substrates is shown in Table 4 (Low and Lee 1997; Orlando *et al.* 2002; Marshall and Wartelle 2004; Namasivayam and Holl 2005; Wartelle and Marshall 2006; Anirudhan *et al.* 2007; Elizalde-Gonzalez *et al.* 2008; Xu *et al.* 2010; Baidas *et al.* 2011; Cao *et al.* 2011; de Lima *et al.* 2012; Wang and Li 2013; Koay *et al.* 2013). However, there is no study that reports on the removal of fluoride using quaternized lignocellulosic fibers.

The objective of this paper was to synthesize quaternized palm kernel shell (QPKS) core fibers adsorbent using the quaternization process and N-(3-chloro-2-hydroxypropyl) trimethylammonium chloride (CHMAC) as the quaternization agent. The parameters investigated in this study included the effects of pH, contact time, sorbent dose, initial

fluoride concentration, adsorption isotherm, and kinetics on the removal of fluoride in aqueous solution using QPKS core fibers.

Table 4. Summary of Reports on Quaternized Lignocellulosic Biomass Used for the Removal of Anionic Substrate

Quaternized biomass	Anionic substrate	q _m (mg/g)	References
Coconut shell	Nitrate	33.7	de Lima <i>et al.</i> 2012
	Sulfate	31.2	
	Phosphate	200.0	
Soybean hull	Arsenate	72.2	Marshall and Wartelle 2004
	Chromate	59.8	
	Dichromate	104.0	
	Phosphate	59.8	
	Selenate	51.0	
Chinese reed	Nitrate	7.6	Namasivayam and Holl 2005
	Perchlorate	13.3	
	Phosphate	16.6	
	Sulfate	10.1	
Coconut coir pith	Arsenic (V)	13.6	Anirudhan <i>et al.</i> 2007
Corn stover	Phosphate	62.7	Wartelle and Marshall 2006
Flax shive	Reactive red 228	190.0	Wang and Li 2013
Giant reed	Perchlorate	150.2	Baidas <i>et al.</i> 2011
Maize cobs	Methyl orange	-	Elizalde-Gonzalez <i>et al.</i> 2008
	Arsenic	-	
Palm kernel shell	Reactive black 5	191.92	Koay <i>et al.</i> 2013
	Reactive red E	182.84	
Rice husk	Reactive blue 2	130.0	Low and Lee 1997
Rice hull	Nitrate	80.0	Orlando, <i>et al.</i> 2002
Sugarcane bagasse	Nitrate	86.8	Orlando, <i>et al.</i> 2002
Rice straw	Sulphate	74.8	Cao <i>et al.</i> 2011
Wheat straw	Acid Red 73	714.3	Xu <i>et al.</i> 2010
	Reactive red 24	285.7	

EXPERIMENTAL

Materials and Methods

Preparation of quaternized palm kernel shell

Raw palm kernel shell waste from crude palm oil production was obtained from the Ulu Langat palm oil mill, Selangor, Malaysia. The PKS was washed with hot water followed by acetone to remove oil, and then dried under the sun for three days. Then, the raw PKS was ground and sieved to a size between 1 and 0.25 mm. The method for quaternization of PKS has been described by Koay *et al.* (2013). Granular PKS was mercerized with sodium hydroxide, NaOH (Merck, 98% purity) of 20 wt.%, 40 wt.%, and 60 wt.% respectively for 10 h to determine the optimum NaOH concentration. Mercerized PKS was rinsed with distilled water and dried at 60 °C for 24 h.

The ratio of the two reactants, namely NaOH and N-(3-chloro-2-hydroxypropyl) trimethylammonium chloride, CHMAC (Sigma, obtained with 60% purity) to PKS was

stoichiometrically calculated from the quaternization reaction (Fig. 2) to yield the optimum quaternization reaction. In this reaction, CHMAC served as the limiting reactant. Therefore, according to the calculation, each gram of PKS reacted with 37 mol of NaOH and 35 mol of CHMAC. The wt./wt. ratio of quaternization reactants, specifically NaOH, CHMAC, and water, was 1.5: 4: 2.5, respectively, per gram of mercerized PKS. The reaction mixture was kept in a sealed container at room temperature for 24 h. Afterwards, the fiber was washed with 0.2% acetic acid solution to stop the reaction and then further washed with distilled water until a neutral pH was achieved. QPKS was dried at 60 °C for 48 h and kept in a desiccator.

Characterization of quaternized palm kernel shell

The QPKS was characterized using carbon, hydrogen, and nitrogen elemental analysis (CHN analysis), a Fourier transform-infrared spectrometer (FT-IR), scanning electron microscope (SEM), energy dispersive X-ray analysis (EDX), Brunauer, Emmett, and Teller analysis (BET), thermogravimetric analysis (TGA), and X-ray diffraction (XRD). The point zero charge, surface chemistry, and chemical composition of QPKS were also determined.

The CHN analysis was conducted to determine the percentage of carbon, hydrogen, and nitrogen contained in the sample. Approximately 0.5 mg of sample was weighed using a CHN C-31 Microbalance. Analysis of the sample was done using a LECO CHNS-932 (USA) spectrometer. Infrared (IR) spectra were recorded by a Perkin Elmer 1750X, FT-IR (Perkin Elmer, USA). The sampling technique used attenuated total reflectance (ATR) for all samples. All spectra were plotted as the percentage of transmittance against wave number (cm^{-1}) at a range of 400 to 4000 cm^{-1} at room temperature. Functional groups of samples were determined from the FTIR spectra.

A Hitachi S-3400N SEM equipped with an EDX attachment (Hitachi, Japan) was operated at 20 to 30 kV. Samples were coated with a thin layer of Au/Pd prior to analysis. The scanning electron photographs were recorded at magnifications of 1000X to 5000X, depending on the nature of the sample. The BET method was used to analyze the surface area of samples. The BET surface area analyzer used was an AutoSorb-1 Quantachrome (Quantachrome Instruments, UK). Pore size distribution, average pore size, and pore volume of the samples were determined using the Barrett, Johner, and Halenda (BJH) equation.

The point zero charge (pHpzc), or the isoelectric point of the samples, was determined by placing 0.1 g of QPKS into 100 mL of 0.01 M NaNO_3 (Acros, 99% purity) solution; pH was adjusted from 2 to 9 by adding 0.1 N HCl (Acros, 99% purity) or 0.1 N NaOH (Merck, 98% purity). The flasks were sealed and shaken for three days at room temperature. The pH of each solution before and after shaking was measured using a pH meter (B729 Eutech-Singapore) (Arockiaraj *et al.* 2014).

Surface chemistry was acquired using the Boehm titration method (Boehm 1994) with the fundamental principle of neutralizing various surface functional groups by acids or bases of different strengths. One gram of sorbent was placed into a 100-mL flask containing 50 mL of 0.1 N Na_2CO_3 (Acros, 99% purity), NaHCO_3 (Acros, 99% purity), NaOH, or HCl. The flasks were sealed and shaken for three days; then, the solution was filtered using 0.45- μm filter paper and 10 mL of the filtrate was pipetted. The acidic solution was titrated with 0.1 N NaOH, and the resulting basic solution was titrated with 0.1 N HCl to determine the remaining acid or base.

Adsorption experiments

A stock solution of fluoride was prepared by dissolving sodium fluoride (MERCK, Germany) in 1 L of double distilled water. The required concentration of fluoride solution was prepared *via* the serial dilution of 100 mg/L fluoride stock solution. All the experiments were completed in batch systems using 250-mL Erlenmeyer flasks. All flasks were sealed properly to prevent leakage and evaporation. All samples were shaken mechanically using a digital orbital shaker (Wise Shake SHO-2D, Korea) at 150 rpm (± 2 rpm) and 25 °C (± 2 °C).

Fluoride ions were measured as per standard methods using a portable fluoride meter (Hach, USA) working at a fixed wavelength of 570 nm. The adsorption performance of QPKS was characterized using fluoride uptake. The adsorption parameters studied were initial pH, contact time, sorbent dose, and initial fluoride concentration. After adsorption, the waste adsorbent can be used as renewable burning material for energy production or incineration.

Effect of initial pH

A pH meter (B729 Eutect, Singapore) was calibrated using buffer solutions of pH 4.0, 7.0, and 10.0 to prevent error. The initial pH of 5 mg/L solutions was adjusted to 1, 2, 3, 4, 5, 6 and 7. After this, 1 g/L of QPKS was added to each flask and they were shaken for 1 h.

Effect of dosage and initial concentration

The effect of QPKS dosage was investigated by running batch experiments with various amounts of QPKS (1, 2, 4, 8, or 10 g/L) added to 100 mL of 5 mg/L fluoride solutions. The pH was adjusted to the optimum pH and the flasks were shaken for 4 h, by which time the solutions had reached equilibrium.

The effect of initial concentration on QPKS adsorption was studied using 100 mL of fluoride solution with initial fluoride concentrations of 5, 10, 20, 30, 40, or 50 mg/L in a series of 250-mL Erlenmeyer flasks (Pyrex, England). A total of 1 g/L of QPKS was added to each flask, which was sealed properly. The samples were shaken for 4 h.

RESULTS AND DISCUSSION

Characterization of Quaternized Palm Kernel Shell

SEM analysis

The textural structure of QPKS was observed with SEM images. Figure 3(b) shows that QPKS had more macropores, which favors the adsorption of larger molecules, as compared with PKS (Fig. 3(a)).

The QPKS has heterogeneous pore arrangement. After quaternization, the surface of the fiber turned smoother because of the dissolution of impurities and lignin under alkaline solution in NaOH. The quantitative data on QPKS pore size was determined using BET analysis in the subsequent part.

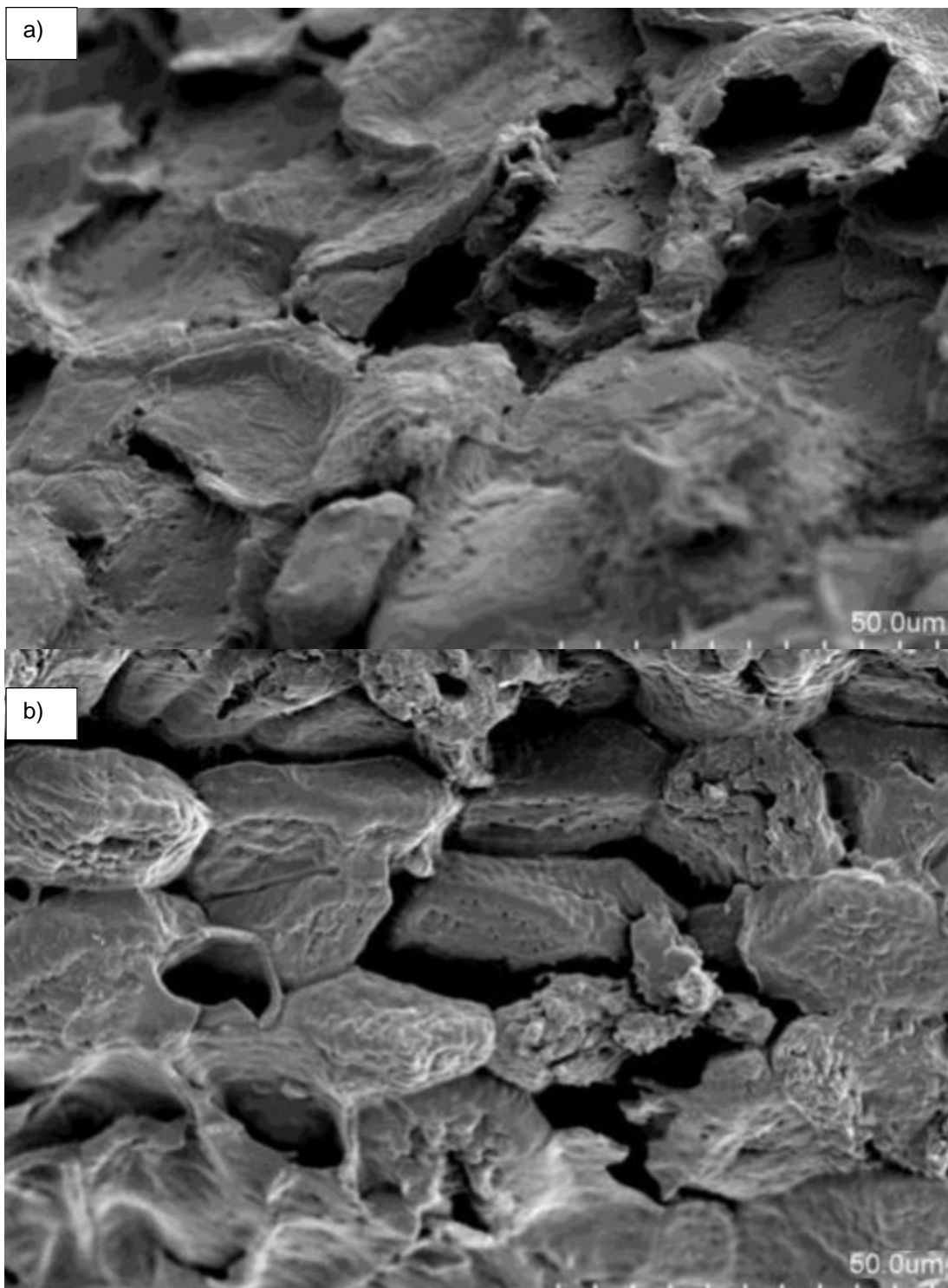


Fig. 3. (a) Palm kernel shell (without quaternization) and (b) quaternized palm kernel shell

BET analysis

As illustrated in Table 5, the average pore diameter of PKS was 2.2 nm, so they can be classified as mesopores. After treatment, QPKS had an average pore diameter of 112.6 nm, classified as macropores. Enlargement of the pore size was due to the dissolution of

lignin and hemicellulose in the NaOH solution during the pre-treatment mercerization process.

Table 5. Textural Characteristics of PKS and QPKS

Samples	SBET (m ² /g)	Average pore diameter (nm)	Pore volume (cm ³ /g)	% of pore volume in stated pore size range (nm)		
				< 2	2-50	>50
PKS	1.932	2.2	0.003	0	64.68	35.32
QPKS	1.717	112.6	0.001	0	0	100

CHN elemental analysis

Results from the CHN elemental analysis tabulated in Table 6 confirmed that the quaternization reaction on PKS was successful. The nitrogen percentage increased from 0.24% to 0.98% after quaternization. According to the CHN analysis, the percentage of carbon in QPKS decreased by 2.16% after treatment. This slight decrease was caused by degradation of lignin, hemicellulose, impurities, and extracts during mercerization and cauterization, with both processes under basic conditions.

Table 6. Elemental Analysis of PKS and QPKS by CHN analyzer

Elemental analysis (%)	PKS (%)	QPKS (%)
Carbon	47.24	45.08
Hydrogen	4.87	5.41
Nitrogen	0.24	0.98

EDX analysis

Energy-dispersive X-ray analysis is a surface elemental analysis used in conjunction with SEM and serves the same purpose as a CHN analysis. However, EDX only detects the surface elements, while CHN analysis detects elements throughout the entire substrate. The results for PKS and QPKS are listed in Table 7, and the spectra are shown in Fig. 4.

Table 7. EDX Analysis of PKS and QPKS

Element (wt.%)	PKS (wt.%)	QPKS (wt.%)
Carbon	43.24	33.94
Oxygen	56.76	47.21
Nitrogen	0.00	13.98

A high percentage of nitrogen was detected in QPKS, but was not detected in PKS. Hence, this analysis again verifies that the quaternary ammonia group (NR₄⁺) reacted on QPKS, resulting in a successful synthesis. Moreover, the percentage of nitrogen in the QPKS sample detected using EDX (13.98%) was higher than results obtained from the CHN analyzer (0.98%). It was therefore concluded that the NR₄⁺ group primarily reacted with the surface of the fiber.

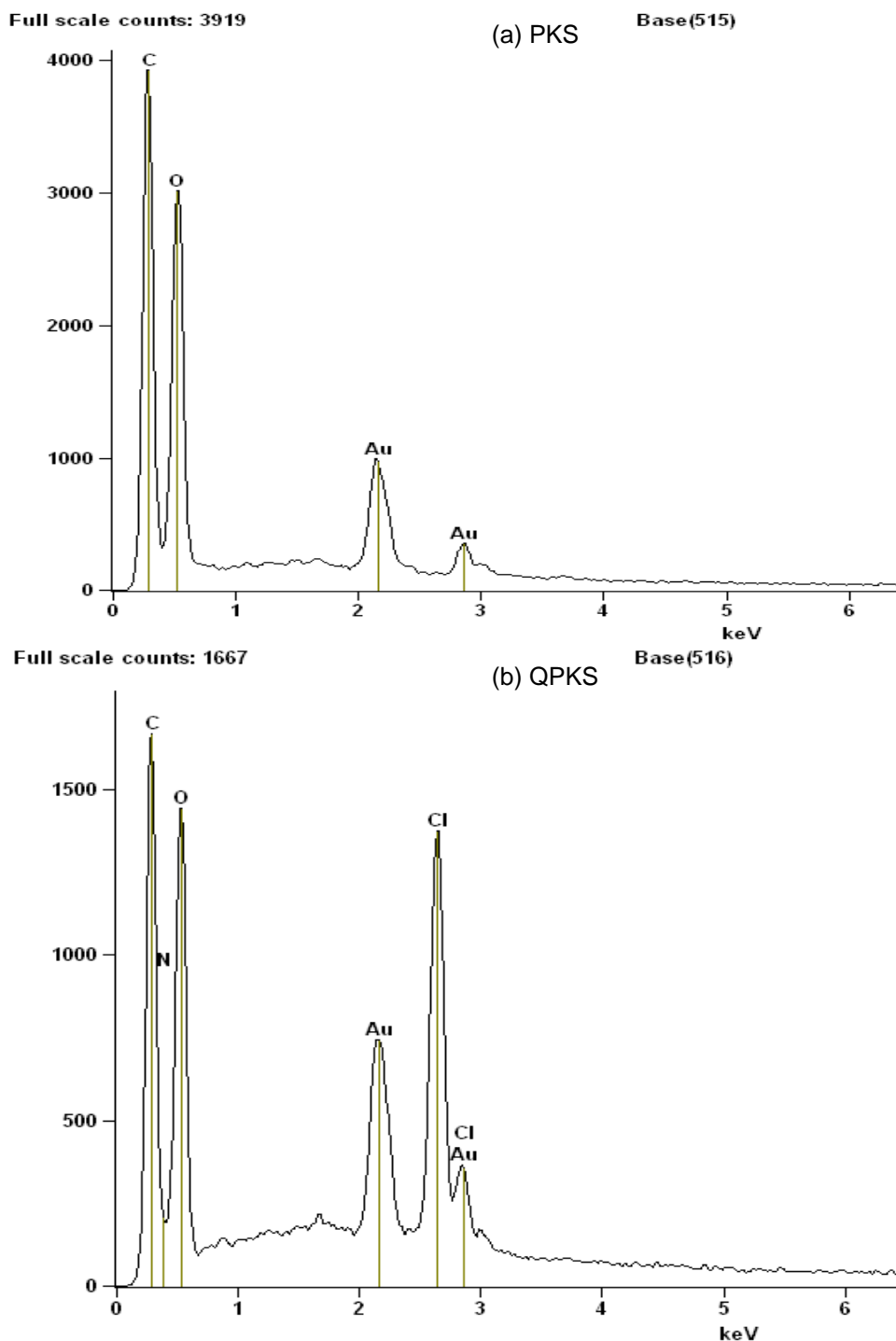


Fig. 4. EDX spectra for (a) PKS and (b) QPKS

FTIR analysis

Figure 5 shows FTIR spectra of PKS and QPKS. A weak peak at 935 cm^{-1} in the QPKS spectrum, which is not present in the PKS spectrum, was attributed to C-N stretching, indicating that the NR_4^+ group was successfully quaternized in QPKS (Hebeish *et al.* 2010). Furthermore, peaks at 1462 and 1420 cm^{-1} with nearly equal intensities, which can be assigned to C-H stretching of the *tert*-butyl group, are evidence of the quaternary ammonia group reacting with QPKS.

The FTIR spectra of PKS and QPKS show O-H stretching at 3353 and 3297 cm^{-1} , and C-H stretching at 2923 and 2902 cm^{-1} , respectively. The C-O stretch mode in C-O-C cellulose linkages appeared at 1030 and 1033 cm^{-1} , respectively, for PKS and QPKS. The PKS spectrum shows weak combination bands between 2500 and 2000 cm^{-1} that are associated with an aromatic ring structure. Furthermore, peaks at 1727 and 1597 cm^{-1} on the PKS spectrum can be attributed to aromatic C=C stretching (Pavia *et al.* 2009).

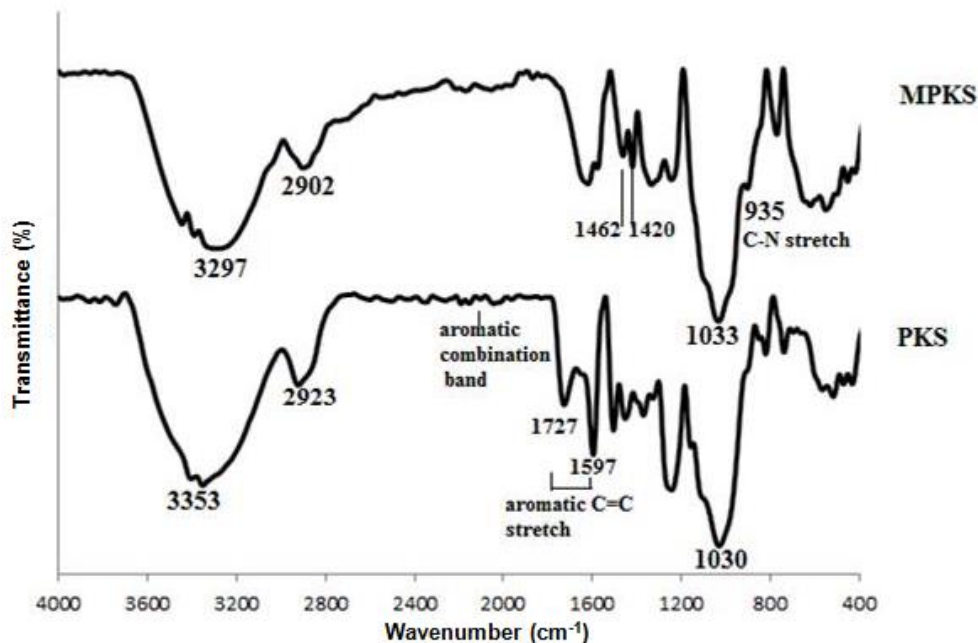


Fig. 5. FTIR spectra of PKS and QPKS

pH_{pzc} of QPKS

From Fig. 6, the pH_{pzc} was determined at a pH of 4.2, where $\Delta\text{pH} = 0$. pH values below the pH_{pzc} resulted in a net positive surface charge of adsorbent. The minimum point, at a pH of 3.2, resulted in the highest positive surface charge for the adsorbent. Hence, a pH of 3.2 was judged to be the best pH condition for removal of anionic substances using QPKS.

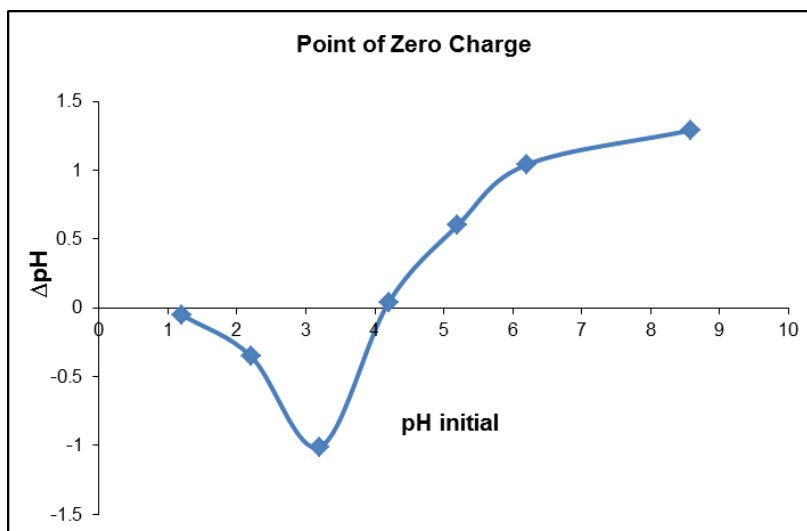


Fig. 6. Point zero charge of QPKS

Surface chemistry

The surface chemistry assessment is designed to distinguish between the surface acidity or basicity of an adsorbent. This information is especially vital for adsorption of charged particles. Oxygen-containing functional groups on adsorbents, such as carboxyl, phenol, and lactone, contribute to surface acidity, whereas Lewis basic functional groups that are proton donating, such as amine groups, contributed to the surface basicity. Increases in the ratio of surface acidity to basicity increase the affinity of the sorbent toward anionic substrates, and *vice versa*. Boehm titration was conducted to test the surface basicity and acidity before and after the PKS surface treatment. The results of Boehm titration for PKS and QPKS are listed in Table 8. The surface total basicity of QPKS increased from 0.652 to 1.132 mmol/g after quaternization treatment. During the quaternization reaction, the NH_4^+ group reacting on QPKS resulted in an increase in surface total basicity in QPKS. Therefore, QPKS acquires a better affinity toward anionic substrates than does untreated PKS.

Table 8. Surface Chemistry Analysis

Surface chemistry (mmol /g)	PKS	QPKS
Carboxyls	1.433	1.477
Lactones	0.067	0.118
Phenols	0.186	0.110
Total acidity	1.686	1.705
Total basicity	0.652	1.132

Effect of pH

Solution pH and ionic strength are the two most influential operational factors controlling the adsorption mechanism. The fluoride removal process is considerably affected by the pH of the sample solution. The effect of pH on the initial solution was investigated, ranging in pH from 1 to 7. The pH of the sample without pH adjustment was measured to be 7.2. The initial concentration used was 5 mg/L, with an adsorbent dosage of 1 g/L for 1 h. Average results from 3 sets of batch experiments were taken for analysis part. As seen in Fig. 7, the percentage of fluoride removed decreased with increasing pH after a pH of 3. This is due to an increased OH^- concentration, which competed with F^- for adsorption. Adsorption is favored at a low pH because of the presence of more protonated sites in the ion exchange with F^- (Nur *et al.* 2014). The actual pH where the fluoride adsorption starts to decrease depends on the surface chemical characteristics of the adsorbent (Loganathan *et al.* 2013). The optimum pH for QPKS was at pH 3, with 63% fluoride removal. Above the pH_{pzc} ($\text{pH} = 4.2$), the adsorbent surface was negatively charged, retarding the diffusion of fluoride ions on the QPKS surface. The decrease in adsorption above the pH_{pzc} was due to the repulsive interaction between anionic fluoride and the adsorbent surface. Similar results for fluoride ion adsorption on other adsorbents have been reported elsewhere (Hiemstra and Van Riemsdijk 2000; Tor *et al.* 2009; Nur *et al.* 2014).

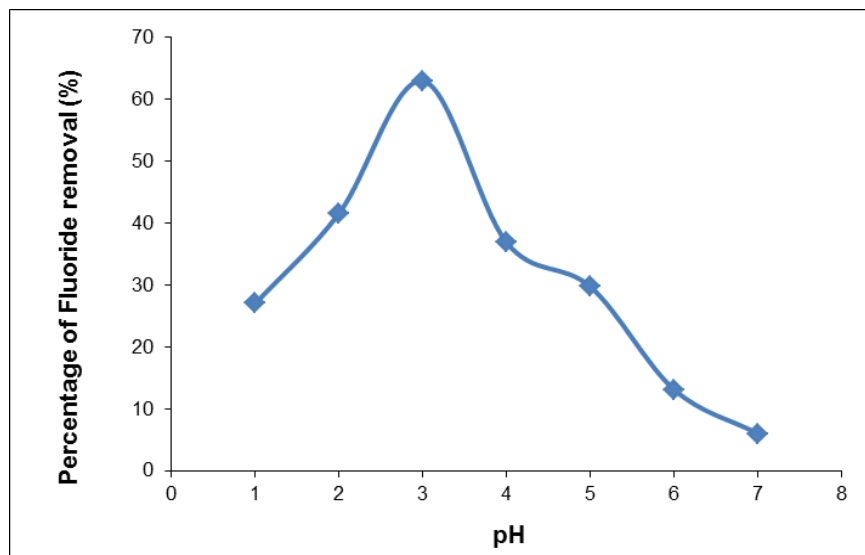


Fig. 7. Effect of pH of fluoride removal on QPKS

Effect of Dosage

The effect of adsorbent dosage was investigated from 1 to 10 g/L at an optimum pH, as shown in Fig. 8. Fluoride removal increased with increasing dosage, and achieved equilibrium at a dose of 8 g/L. This increase in load capacity is due to the availability of a higher number of fluoride ions per unit mass of adsorbent, *i.e.*, a higher fluoride/adsorbent ratio. However, further increases in adsorbent dose did not show any appreciable improvement in fluoride removal. This may be because of the very low equilibrium concentration of fluoride, *i.e.*, the driving force responsible for adsorption became negligible (Kumar *et al.* 2012).

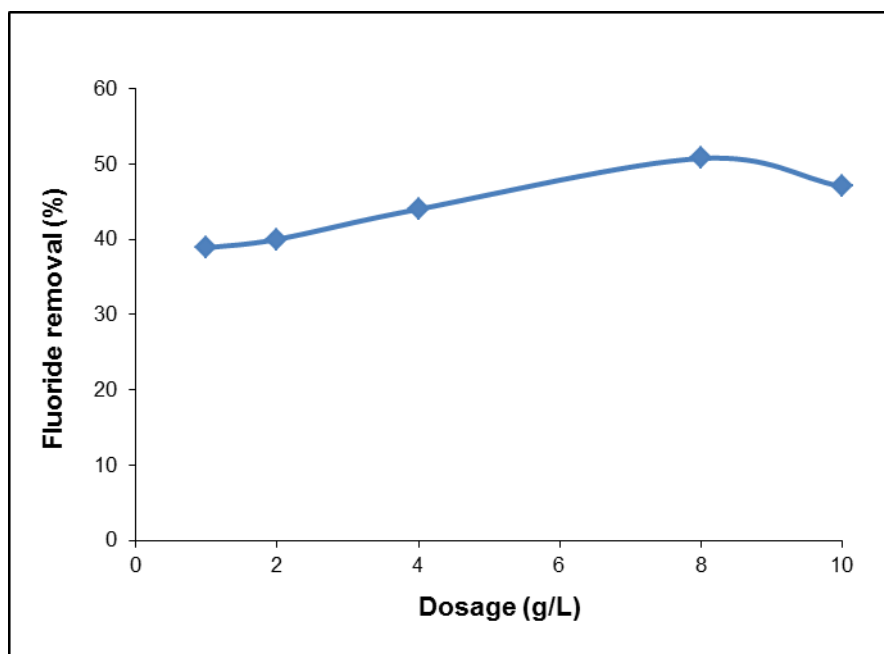


Fig. 8. Effect of dosage for fluoride removal on QPKS

Effects of Initial Concentration and Contact Time

Contact time studies are essential to explore the equilibration time in the adsorption process. The contact time studies for fluoride adsorption on QPKS at various initial fluoride concentrations are presented in Fig. 9.

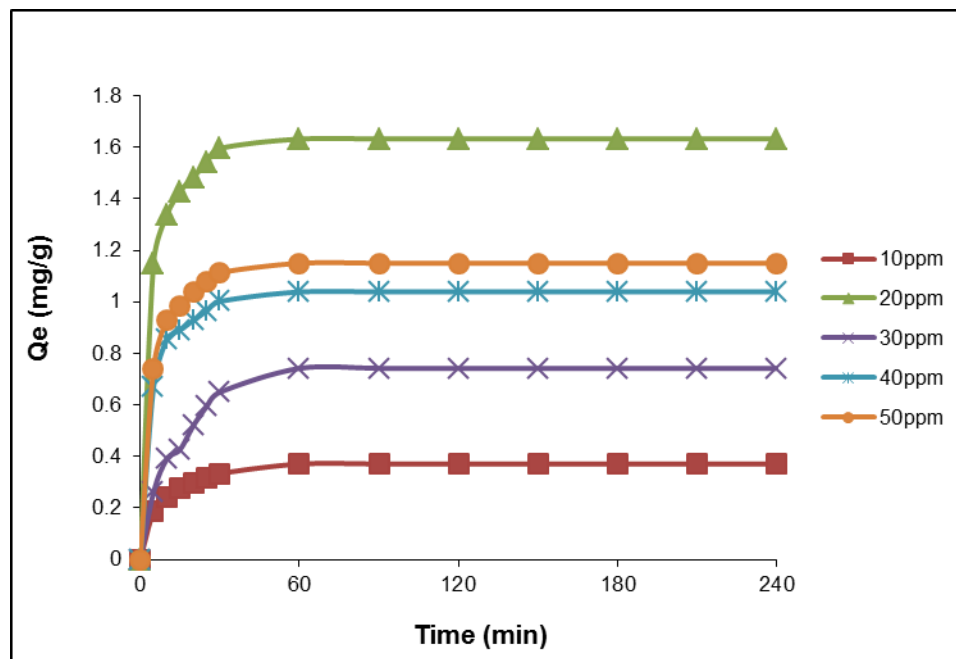


Fig. 9. Effect of initial concentration and contact time (QPKS dosage: 8 g/L, pH: 3, temperature: 25 °C)

The adsorption curves in Fig. 9 are smooth and continuous. Initially, fast fluoride adsorption was observed in QPKS, confirming the chemical nature of the adsorption process; however, it eventually slowed down and attained equilibrium with time. The initial concentration was varied from 10 to 50 mg/L at an optimum pH and an adsorbent dosage, with a contact time of 4 h. The highest adsorption capacity which is the Q_e was achieved with an initial concentration of 20 mg/L, which was close to 1.7 mg/g, with a 63% fluoride removal. This is probably due to the increase in the mass transfer driving force, resulting in a higher loading capacity for QPKS, as its active sites were occupied by a larger amount of fluoride ions. The adsorption process was rapid for the first 30 min, and equilibrium was achieved after 60 min. The increase in fluoride adsorption capacity on QPKS can be attributed to the formation of surface functional groups after quaternization, as the active sites caused an appreciable increase in adsorption.

Adsorption isotherms

An adsorption isotherm is a study of the adsorbent-adsorbate interaction in an equilibrium state, which leads to a fundamental understanding of the adsorption process, such as a monolayer or a multilayer adsorption, maximum adsorption capacity, or the degree of heterogeneity on adsorbate surfaces, which consequently helps in designing an efficient adsorption system. Equation 1 shows the calculation of the amount of adsorbate adsorbed per gram of adsorbent in an equilibrium condition (q_e),

$$q_e = \frac{(C_0 - C_e)V}{m} \quad (1)$$

where C_0 and C_e (mg/L) are the initial and final concentrations of adsorbate in bulk solution, V (L) is the volume of the solution, and m (g) is the mass of the adsorbent. Four isotherm models, *i.e.*, Langmuir, Freundlich, Sips, and Redlich-Peterson isotherms, were used to analyze the data. A non-linear method was chosen over a linear method to eliminate the inherent bias resulting from linearization.

The Langmuir isotherm model (Eq. 2) assumes that adsorption is a monolayer at homogeneous surfaces. One active site only traps one adsorbate molecule, and there is no interaction between the molecule adsorbed and the neighboring site. Hence, the adsorbent has a finite capacity at the saturation point where no more adsorption can occur (Langmuir 1916),

$$q_e = \frac{K_L C_e}{1 + \alpha_L C_e} \quad (2)$$

where q_e is the amount of adsorbate adsorbed on each gram of adsorbent at equilibrium, C_e is the concentration of adsorbate in solution at equilibrium, and K_L and α_L are Langmuir constants.

The Freundlich isotherm model (Eq. 3) describes multilayer adsorption onto heterogeneous surfaces. K_F is the Freundlich constant and $1/n_F$ is the heterogeneity factor. If a value of $1/n_F$ is closer to zero, the degree of surface heterogeneity becomes higher on the adsorbent, and *vice versa*. If the value of $1/n_F$ equals unity, the adsorption is linear. If $1/n_F < 1$, then chemisorption is more favorable. If $1/n_F > 1$, then physisorption is more favorable (Haghsresht and Lu 1998),

$$q_e = K_F C_e^{1/n_F} \quad (3)$$

where q_e is the amount of adsorbate per gram of adsorbent at equilibrium, C_e is a concentration of adsorbate in solution at equilibrium, and K_F and n_F are Freundlich constants.

The Sips isotherm model (Eq. 4) is a blending of the Langmuir and Freundlich isotherm models; hence, it is more advanced in defining a heterogeneous surface. Unlike Langmuir and Freundlich isotherm models, the Sips isotherm model has three parameters, which are K_s , α_s , and n_s . At low concentrations, the Sips isotherm follows the Freundlich isotherm model, whereas at high concentrations, it follows the Langmuir isotherm model (Sips 1948). If $1/n_s \ll 1$, the surface of the adsorbent is heterogeneous, and when $1/n_s \approx 1$, the surface of the adsorbent is homogenous.

$$q_e = \frac{K_S C_e^{1/n_S}}{1 + \alpha_S C_e^{1/n_S}} \quad (4)$$

where q_e is amount of adsorbate per gram of adsorbent at equilibrium, C_e is a concentration of the adsorbate in solution at equilibrium, and K_s , α_s , and n_s are Sips constants.

The Redlich-Peterson isotherm model (Eq. 5) is a versatile model that combines fundamentals from both the Langmuir and Freundlich isotherm models. It has three constants (K_R , α_R , and β) that are similar to the Sips isotherm model, in which adsorption is hybrid and can be applied over a wide concentration range, regardless of the surface condition. The constant β is an exponent that lies between 0 and 1. However, at high concentrations where $0 < \beta < 1$, it approaches the Freundlich isotherm model, and at low

concentrations, when the β value is close to one, it approaches the Langmuir isotherm model which is opposite from Sips's isotherm model (Redlich and Peterson 1959),

$$q_e = \frac{K_R C_e}{1 + \alpha_R C_e^\beta} \quad (5)$$

where q_e is the amount of adsorbent per gram of adsorbent at equilibrium, C_e is a concentration of adsorbate in solution at equilibrium, and K_R , α_R , and β are Redlich-Peterson constants.

The isotherm constant values with regression coefficients for all four models are listed in Table 9. The experimental adsorption capacity and the adsorption capacity predicted by isotherm models were compared, and the results are presented in Fig. 10.

Table 9. Values of Constants for Isotherm Models

Isotherm	Langmuir	Freundlich	Redlich-Peterson	Sips
	$K_L = 0.3235$	$K_F = 0.4929$	$K_{RP} = 337.2659$	$K_S = 0.4929$
	$\alpha_L = 0.1480$	$1/n_F = 0.3982$	$\alpha_{RP} = 683.6067$	$1/n_S = 0.3982$
Parameters		$n_F = 2.5113$	$\beta = 0.6020$	$n_S = 2.5113$
				$\alpha_S = 0$
	$R^2 = 0.9241$	$R^2 = 0.9716$	$R^2 = 0.9716$	$R^2 = 0.9716$
	SSE = 0.0419	SSE = 0.0157	SSE = 0.0157	SSE = 0.0157

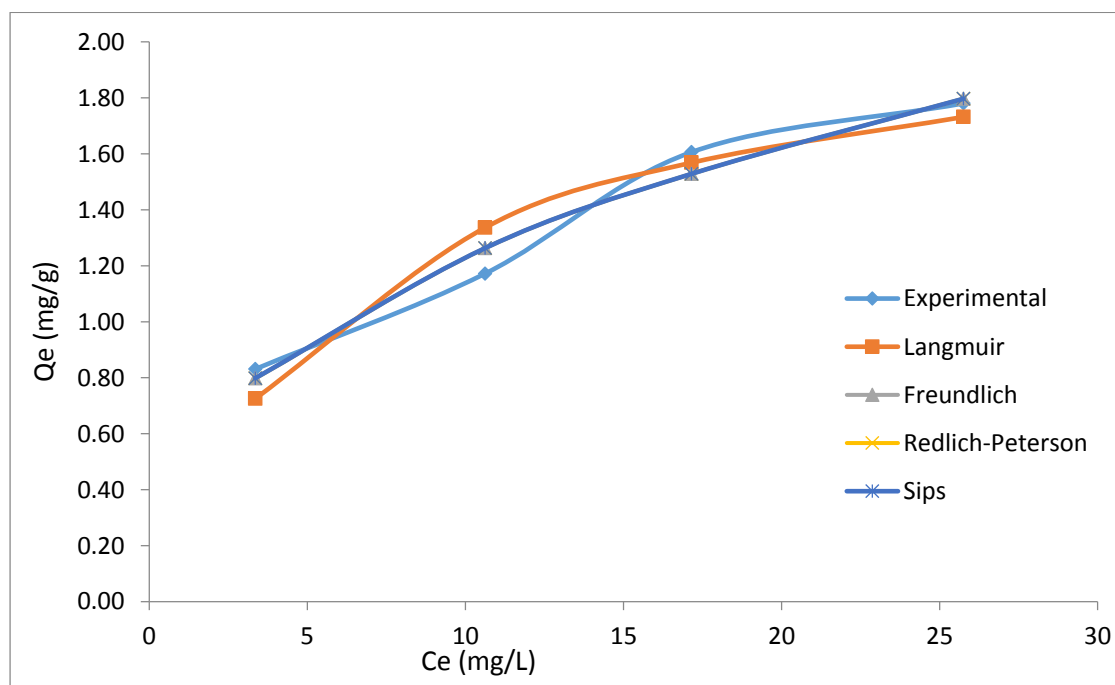


Fig. 10. Isotherm models for fluoride removal on QPKS

Table 9 shows comparisons of the four isotherms applied in this adsorption study. The amount of fluoride adsorbed per unit mass of QPKS (q_e) was plotted against the concentration of fluoride remaining in solution (C_e). The Freundlich, Sips, and Redlich-Peterson ($R^2 = 0.9716$) isotherms seemed to be better-fitting models than the Langmuir (R^2

= 0.9241) isotherm. The use of a coefficient of determination of linear regression analysis for determining the best-fitting of the different linear isotherms was found not to be appropriate. Further analysis of the non-linear method was attempted. A computer operation application was developed to determine the isotherm parameters using an optimization routine to maximize the coefficient of determination between the experimental data and isotherms in the solver add in Microsoft Excel. Figure 10 shows that the Freundlich, Redlich–Peterson, and Sips isotherms overlapped, and seemed to be the best-fitting models with the same regression coefficient values ($R^2 = 0.9716$). Unlike a linear analysis, different isotherm forms affected the value of R^2 , and impacted the final determination of parameters, where nonlinear methods would prevent such errors (Ho *et al.* 2002).

The value of $1/n_F$ in the Freundlich isotherm was 0.3982 (< 1), which indicated that chemisorption was more likely to take place in this adsorption. The degree of surface heterogeneity also appeared to be higher on the adsorbent. This led to a strong interaction between the adsorbate (fluoride) and the QPKS surface, thus creating ionic bonds. The value of $1/n_s$ from Sips isotherm is less than 1 and further confirms adsorption on the surface of QPKS is heterogeneous. The value of Redlich–Peterson's β value was 0.602, which meant the isotherms were approaching Freundlich's but not Langmuir's isotherm. It has been previously reported that Freundlich's isotherm is a special case of Redlich–Peterson's isotherm when constants K_R and α_R are much greater than unity (Ho 2004).

Adsorption Kinetics

Pseudo-first-order rate and pseudo-second-order rate equations

Kinetics studies of adsorption help to understand the removal rate, mechanism of adsorption, and rate determination steps of the adsorption process. The pseudo-first kinetic and pseudo-second order kinetics models (Ho and McKay 1999) are the simplest kinetics models for describing any adsorption reaction.

Lagergren (1898) presented a first-order rate equation to describe the process of liquid-solid phase adsorption of oxalic acid and malonic acid onto charcoal, which is believed to be the earliest model pertaining to the adsorption rate based on the adsorption capacity. In 1998, Ho described a process of adsorption of divalent metal ions onto peat (Ho and McKay 1998), in which the chemical bonding among divalent metal ions and polar functional groups on peat, such as aldehydes, ketones, acids, and phenolics, were responsible for the cation-exchange capacity of the peat. Ho's second-order rate equation has been called the pseudo-second-order rate equation to distinguish it from kinetic equations based on adsorption capacity from concentration of solution (Ho 2006). Equation 6 illustrates the pseudo-first kinetic model, and Eq. 7 shows the pseudo-second order kinetic model:

$$q_t = q_{e1}(1 - e^{-k_1 t}) \quad (6)$$

$$q_t = \frac{t}{\left(\frac{1}{k_2 q_{e2}^2}\right) + \left(\frac{t}{q_{e2}}\right)} \quad (7)$$

where k_1 and k_2 (min^{-1} and $\text{g} / \text{mg} \cdot \text{min}$) are the pseudo-first and pseudo-second order rate constants, respectively, and q_{e1} and q_{e2} (mg/g) are the calculated values of the amount of adsorbent adsorbed per gram of adsorbent in an equilibrium state by the pseudo-first and pseudo-second order kinetics models, respectively. The q_t (mg/g) is the amount of

adsorbent adsorbed per gram of adsorbent during time, t . The q_e (mg/g) is the experimental value of adsorbent adsorbed per gram of adsorbent.

The results are shown in Table 10 and Fig. 11. The coefficient of determination, R^2 , for the pseudo second-order adsorption model had a high value (0.999) for all concentrations of fluoride in this study. Similar results were obtained by Liu *et al.* (2002) for the adsorption of fluoride onto ion-exchange fiber and by Fan *et al.* (2003) on low-cost materials.

Table 10. Kinetics Parameters for Adsorption of Fluoride on QPKS

Kinetics model	Parameter	Initial concentration of fluoride ion (mg/L)				
		10	20	30	40	50
Pseudo first order	K_1	0.0617	0.0951	0.0640	0.0831	0.0896
	R^2	0.9942	0.9650	0.9683	0.9683	0.9849
Pseudo second order	K_2	0.0869	0.0531	0.0243	0.0689	0.0635
	R^2	0.9995	0.9999	0.9984	0.9999	0.9999
Intraparticle diffusion (Weber-Morris)	K_i	0.8672	0.3580	0.7540	0.9462	1.0560
	R^2	0.9465	0.9821	0.9178	0.9880	0.9753
Elovich	α	0.4671	3.8361	1.1426	1.9785	2.1217
	β	2.7933	0.9470	1.0569	1.3263	1.1531
	R^2	0.9821	0.9753	0.9880	0.9178	0.9465

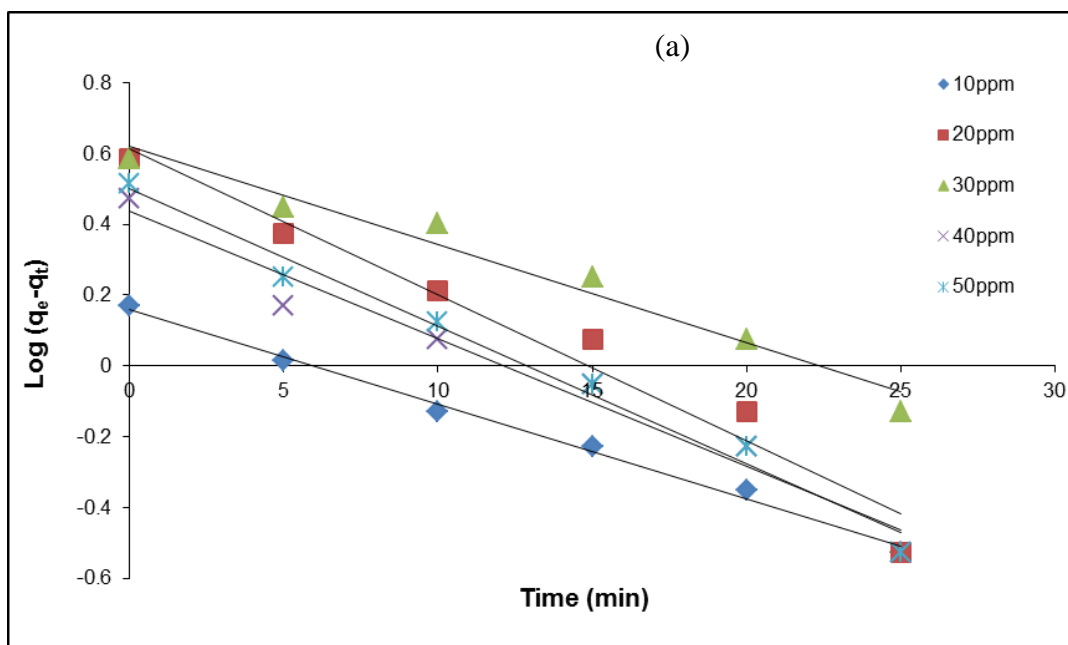


Fig. 11. (a) Pseudo-first order kinetics plots at various initial concentrations of fluoride (QPKS dosage: 8 g/L, pH: 3, and temperature: 25 °C)

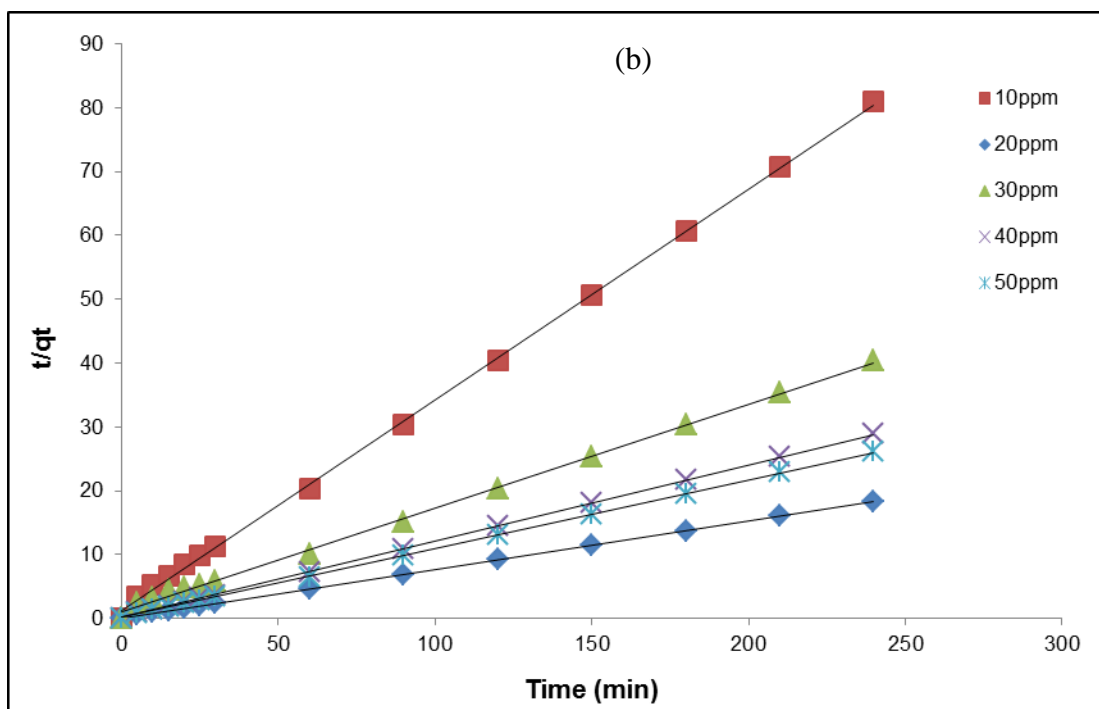


Fig. 11. (b) Pseudo-second order kinetics plots at various initial concentrations of fluoride (QPKS dosage: 8 g/L, pH: 3, and temperature: 25 °C)

Elovich's equation

A kinetic equation of chemisorption was established previously by Zeldowitsch (1934) and was used to describe the rate of adsorption of carbon monoxide on manganese dioxide, which decreases exponentially with an increase in the amount of gas adsorbed. This so-called Elovich equation is expressed as follows,

$$\frac{dq_t}{dt} = \alpha e^{-\beta q_t} \quad (8)$$

where β is related to the extent of surface coverage and activation energy for chemisorption and α is the initial sorption rate (mg/g min). The Elovich equation was applied to determine the kinetics of chemisorption of gases onto heterogeneous solids (Rudzinski and Panczyk 2000). With the assumption of $\alpha\beta t \gg 1$ (Chien and Clayton 1980), Eq. 8 was integrated with the kinetic rate equation with same boundary condition of $q = 0$ at $t = 0$, and $q_t = q$ at $t = t$, to yield:

$$q = \frac{1}{\beta} \ln(\alpha \beta) + \frac{1}{\beta} \ln t \quad (9)$$

The Elovich equation has also been used to describe the adsorption process of pollutants from aqueous solutions (Cheung *et al.* 2001; Sag and Aktay 2002).

It has been suggested that diffusion may account for the Elovich kinetic pattern, and conformation to this equation alone might be taken as evidence that the rate-determining step is a diffusion process in nature. The kinetics curve of sorption demonstrated a good fit with the model ($R^2 > 0.97$), which may indicate that diffusion rate-limiting is more prominent in fluoride sorption using QPKS at lower initial concentrations (10, 20, and 30 mg/L) (Fig. 12).

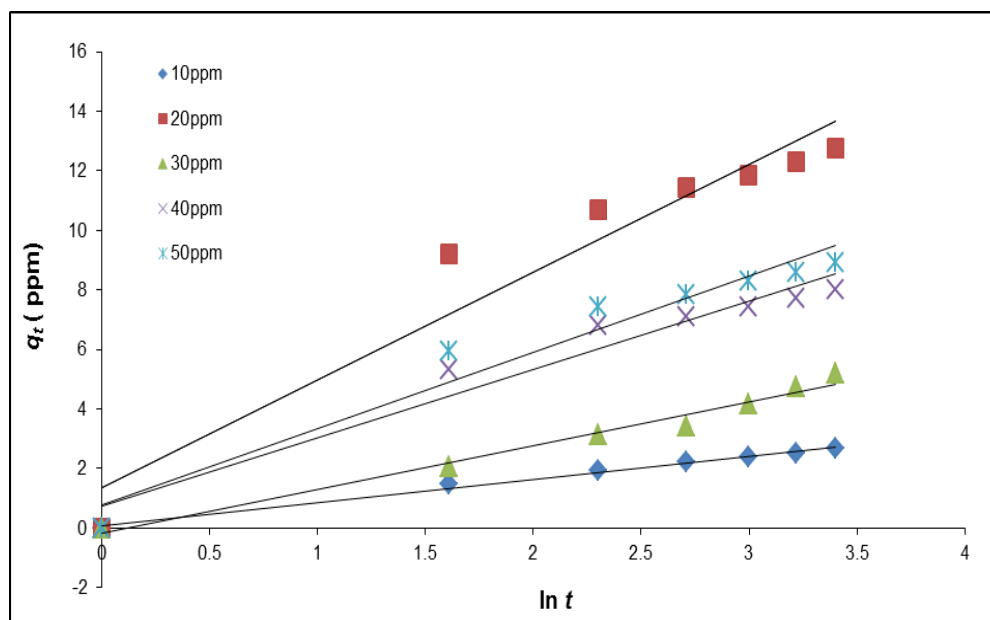


Fig. 12. Elovich kinetics plots with various initial concentrations of fluoride (QPKS dosage: 8 g/L, pH: 3, and temperature: 25 °C)

The general explanation for this form of kinetics law involves a variation of the energetics of chemisorption with the active sites that are heterogeneous quaternized palm kernel shell (QPKS) fibers and therefore exhibit different activation energies for chemisorption (Ozacar and Sengil 2005) because the cell walls of QPKS mostly consist of cellulose, lignin, and hydroxyl groups. The Elovich model gives a good correlation for adsorption on highly heterogeneous surfaces and also shows that along with surface adsorption, chemisorption is an additionally occurring dominant phenomenon. However, in a highly heterogeneous system of surface adsorption, chemisorptions, ion exchange, precipitation, and intra-particle diffusion also occur concurrently. It was not possible to find which process was dominant. Elovich equation correlation coefficients were lower than those of the pseudo second-order equation. The Elovich equation does not predict any definite mechanism, but it is useful in describing adsorption on highly heterogeneous adsorbents. The adsorption system obeys the pseudo second-order kinetics model for the entire adsorption period and thus supports the assumption behind the model that the adsorption is due to chemisorption. These results imply that the chemisorption mechanism may play an important role in the adsorption of fluoride onto QPKS fibers. The adsorption of fluoride onto QPKS fibers most likely takes place *via* surface exchange reactions until the surface functional sites are fully occupied. After this, fluoride molecules diffuse into QPKS fiber pores for further interactions and/or reactions such as ion-exchange and complexation interactions (Ornek *et al.* 2007; Riahi *et al.* 2009). Thus, the adsorption of fluoride onto QPKS fibers is very well explained by the pseudo-second-order model. This result is consistent with other studies related to fluoride removal using adsorption (Chakrapani *et al.* 2010; Mohammad *et al.* 2013).

Intraparticle diffusion model

The possibility that diffusion might be the only rate-determining step of this adsorption was judged by the linear dependence of Weber-Morris (1963):

$$q_t = k_i t^{0.5} + C \quad (12)$$

where C is a coefficient accounting for the bonding effect between the layers; *i.e.*, as the value of C increases, so does the boundary layer effect. k_i is the rate constant of the process, $\text{mg g}^{-1} \text{min}^{-1/2}$.

If the experimental data describe a multilinear dependence, this means that the sorption is influenced by two or more rate-determining steps, *i.e.*, the process is occurring in the transition region. The intra-particle diffusion rates (k_i) were determined from plots of q_t versus $t^{0.5}$. If intra-particle diffusion is a rate controlling step, then the plots should be linear and pass through the origin.

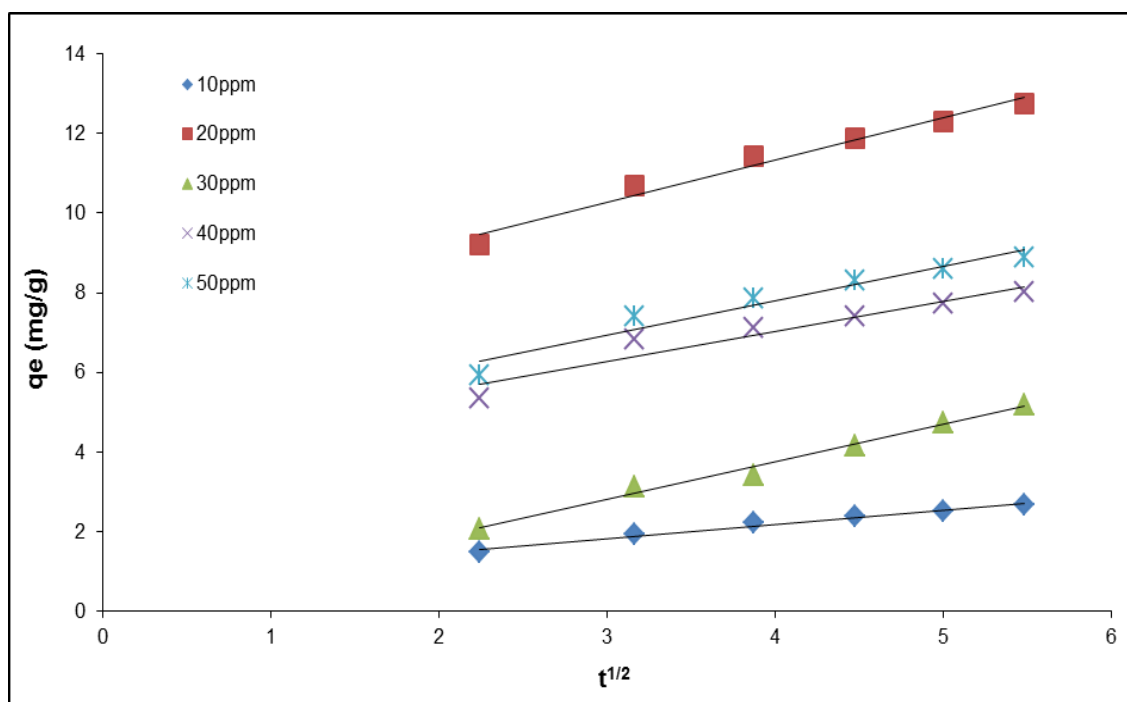


Fig. 13. Intraparticle diffusion kinetics plots with various initial concentrations of fluoride (QPKS dosage: 8 g/L, pH: 3, and temperature: 25 °C)

Figure 13 and Table 10 depict intraparticle diffusion as moderate, and the slope of the linear portion of the curve at each solute concentration gives the value of K_i . This result suggests that the adsorption is governed by diffusion within the pores of the adsorbent. The linear portions of the curves do not pass through the origin (Fig. 13), indicating that the mechanism for fluoride removal on QPKS may be complex, and both surface adsorption and intraparticle diffusion contribute to the absorption rate.

Comparison with other adsorbent

Defluoridation using other adsorbents from previous study has been compared with this study.

Table 11 shows the comparison between fluoride removal capacity with different fluoride initial concentration used using different plant-based adsorbents. Fluoride removal capacity from this study shows an acceptable value with other adsorbents.

Table 11. Comparison of Various Plant-based Adsorbents for Removal of Fluoride in Aqueous Solution (Bashir *et al.* 2015).

Plant-based adsorbent	Fluoride concentration range (mg/ml)	Adsorption capacity (mg/g)	Reference
Activated bagasse carbon	2.5-15	1.15	Yadav <i>et al.</i> 2013
Chemically modified palm kernel shell	2.5-15	2.35	Bashir <i>et al.</i> 2015
Corn stover biochar	1-100	6.42	Mohan <i>et al.</i> 2014
Magnetic corn stover biochar	1-100	4.11	Mohan <i>et al.</i> 2014
<i>Moringa oleifera</i>	1-10	2.057	Parlikar and Mokashi 2013
<i>Pleurotus eryngii</i> (Fungus)	5-25	0.244	Amin <i>et al.</i> 2014
<i>Pleurotus ostreatus</i>	5-25	1.27	Ramanaiah <i>et al.</i> 2007
Quaternized palm kernel shell (QPKS)	10-50	1.7	This study
Rice husk	0-400	0.82	Vardhan and Karthikeyan 2011
Sawdust	2.5-15	1.74	Yadav <i>et al.</i> 2013
Tea ash	1.5-50	2.05-9.42	Mondal <i>et al.</i> 2012
Tea waste	5-100	0.988	Cai <i>et al.</i> 2015
Wheat straw	2.5-15	1.93	Yadav <i>et al.</i> 2013

CONCLUSIONS

1. The use of quaternized palm kernel shell (QPKS) as an alternative low-cost adsorbent has been shown to have very good potential for the removal of fluoride ions from aqueous solution. The adsorption process was influenced by parameters such as adsorbent dosage, initial concentration, and pH.
2. Batch experiments demonstrated that the maximum fluoride removal by QPKS occurred at pH 3. The adsorption equilibrium data were fitted with Langmuir, Freundlich, Redlich-Peterson, and Sips isotherm models. The adsorption of fluoride was best represented by Freundlich, Redlich-Peterson, and Sips models, with an R^2 value of 0.97.
3. Kinetics data for adsorption of fluoride using QPKS tended to fit well in pseudo-second-order Lagergren kinetics models.

ACKNOWLEDGMENTS

The authors would like to acknowledge the financial support from the Research University Grant Scheme (RUGS) from Universiti Putra Malaysia Project no:05-02-12-2203RU and High Impact Research MoE Grant: UM.C/625/1/HIR/MoE/52 from the Ministry of Education Malaysia, RU022A-2014, for the success of this project.

REFERENCES CITED

- Amin, F., Talpur, F., Balouch, A., Surhio, M., and Bhutto, M. (2014). "Biosorption of fluoride from aqueous solution by white-rot fungus *Pleurotus eryngii* ATCC 90888," *Environmental Nanotechnology, Monitoring & Management* 3, 30-37. DOI: 10.1016/j.enmm.2014.11.003
- Anirudhan, T. S., Unnithan, M. R., Divya, L., and Senan, P. (2007). "Synthesis and characterization of polyacrylamide-grafted coconut coir pith having carboxylate functional group and adsorption ability for heavy metal ions," *J. Appl. Polym. Sci.* 104(6), 3670-3681. DOI: 10.1002/app.25002
- Arockiaraj, I., Karthikeyan, S., and Renuga, V. (2014). "Effects of various carbonization processes in the preparation of nanoporous carbon materials using *Ipomoea carnea* stem waste for the removal of dyes from textile industrial effluents," *J. Environ. Nanotechnol.* 3(2), 9-21. DOI : 10.13074/jent.2013.03.142064
- Baidas, S., Gao, B., and Meng, X. (2011). "Perchlorate removal by quaternary amine modified reed," *J. Hazard. Mater.* 189(1), 54-61. DOI:10.1016/j.jhazmat.2011.01.124
- Bashir, M., Salmiaton, A., Nourouzi, M., Azni, I., and Harun, R. (2015). "Fluoride removal by chemical modification of palm kernel shell-based adsorbent: A novel agricultural waste utilization approach," *Asian J. of Microbial. Biotech. Env. Sc.* 17(3), 533-542.
- Bhatnagar, A., Kumar, E., and Sillanpaa, M. (2011). "Fluoride removal from water by adsorption - A review," *Chem. Eng. J.* 171(3) 811-840. DOI: 10.1016/j.cej.2011.05.028
- Boehm, H. P. (1994). "Some aspects of the surface chemistry of carbon blacks and other carbons," *Carbon* 32(5), 759-769. DOI:10.1016/0008-6223(94)90031-0
- Cai, H., Chen, G., Peng, C., Zhang, Z., Dong, Y., Shang, G., Zhu, X., Gao, H., and Wan, X. (2015). "Removal of fluoride from drinking water using tea waste loaded with Al/Fe oxides: A novel, safe and efficient biosorbent," *Applied Surface Science.* 328,34-44. DOI: 10.1016/j.apsusc.2014.11.164
- Cao, W., Dang, Z., Zhou, X. Q., Yi, X. Y., Wu, P. X., Zhu, N.-W., and Lu, G. N. (2011). "Removal of sulphate from aqueous solution using modified rice straw: Preparation, characterization and adsorption performance," *Carbohydr. Polym.* 85(3), 571-577. DOI: 10.1016/j.carbpol.2011.03.016
- Chakrapani, C. H., Suresh Babu, C. H., Vani, K. N. K., and Somasekhara Rao, K. (2010). "Adsorption kinetics for the removal of fluoride from aqueous solution by activated carbon adsorbents derived from the peels of selected citrus fruits," *E-J. Chem.* 7(S1), S419-S427. DOI: 10.1155/2010/582150
- Cheung, C. W., Porter, J. F., and McKay, G. (2001). "Sorption kinetic analysis for the removal of cadmium ions from effluents using bone char," *Water Res.* 35(3), 605-612. DOI: 10.1016/S0043-1354(00)00306-7
- Chien, S. H. and Clayton, W. R. (1980). "Application of Elovich equation to the kinetics of phosphate release and sorption in soils," *Soil Sci. Soc. Am. J.* 44(2), 265-268. DOI: 10.2136/sssaj1980.03615995004400020013x
- de Lima, A. C. A., Nascimento, R. F., de Sousa, F. F., Filho, J. M., and Oliveira A. C. (2012). "Modified coconut shell fibers: A green and economical sorbent for the removal of anions from aqueous solutions," *Chem. Eng. J.* 185, 274-284. DOI: 10.1016/j.cej.2012.01.037

- Deng, S., Liu, H., Zhou, W., Huang, J., and Yu, G. (2011). "Mn–Ce oxide as a high-capacity adsorbent for fluoride removal from water," *J. Hazard. Mater.* 186(2), 1360-1366. DOI: 10.1016/j.jhazmat.2010.12.024
- Dissanayake, C. B. (1991). "The fluoride problem in the ground water of Sri Lanka – Environmental management and health," *Int. J. Environ. Stud.* 38(2-3), 137-155. DOI: 10.1080/00207239108710658
- Elizalde-González, M. P., Mattusch, J., and Wennrich, R. (2008). "Chemically modified maize cobs waste with enhanced adsorption properties upon methyl orange and arsenic," *Bioresour. Technol.* 99(11), 5134-5139. DOI:10.1016/j.biortech.2007.09.023
- Fan, X., Parker, D., and Smith, M. D. (2003). "Adsorption kinetics of fluoride on low cost materials," *Water Res.* 37(20), 4929-4937. DOI: 10.1016/j.watres.2003.08.014
- Gupta, V. K., and Suhas. (2009). "Application of low-cost adsorbents for dye removal - A review," *J. Environ. Manage.* 90(8), 2313-2342. DOI:10.1016/j.jenvman.2008.11.017
- Haghseresht, F., and Lu, G. Q. (1998). "Adsorption characteristics of phenolic compounds onto coal-reject-derived adsorbents," *Energy Fuels* 12(6), 1100-1107. DOI: 10.1021/ef9801165
- Hebeish, A., Higazy, A., El-Shafei, A., and Sharaf, S. (2010). "Synthesis of carboxymethyl cellulose (CMC) and starch-based hybrids and their applications in flocculation and sizing," *Carbohydrate Polymers* 79(1),60-69. DOI:10.1016/j.carbpol.2009.07.022
- Hichour, M., Persin, F., Sandeaux, J., and Gavach, C. (1999). "Fluoride removal from waters by Donnan dialysis," *Sep. Purif. Technol.* 18(1), 1-11. DOI: 10.1016/S1383-5866(99)00042-8
- Hiemstra, T., and Van Riemsdijk, W. H. (2000). "Fluoride adsorption on goethite in relation to different types of surface sites," *J. Colloid Interf. Sci.* 225(1), 94-104. DOI: 10.1006/jcis.1999.6697
- Ho, Y. S. (2004). "Selection of optimum adsorption isotherm," *Carbon* 42(10), 2115-2116. DOI: 10.1016/j.carbon.2004.03.019
- Ho, Y. S. (2006). "Review of second-order models for adsorption systems," *J. Hazard. Mater.* 136(3), 103-111. DOI: 10.1016/j.jhazmat.2005.12.043
- Ho, Y. S., and McKay, G. (1998). "Sorption of dye from aqueous solution by peat," *Chem. Eng. J.* 70(2), 115-124. DOI: 10.1016/S0923-0467(98)00076-1
- Ho, Y. S., and McKay, G. (1999). "Pseudo-second order model for sorption processes," *Process Biochem.* 34(5), 451-465. DOI: 10.1016/S0032-9592(98)00112-5
- Ho, Y. S., Huang, C. T., and Huang, H. W. (2002). "Equilibrium sorption isotherm for metal ions on tree fern," *Process Biochem.* 37(12), 1421-1430. DOI: 10.1016/S0032-9592(02)00036-5
- Idris, S. S., Rahman, N. A., and Ismail, K. (2012). "Combustion characteristics of Malaysian oil palm biomass, sub-bituminous coal and their respective blends via thermogravimetric analysis (TGA)," *Bioresour. Technol.* 123, 581-591. DOI: 10.1016/j.biortech.2012.07.065
- Kagne, S., Jagtap, S., Dhawade, P., Kamble, S. P., Devotta, S., and Rayalu, S. S. (2008). "Hydrated cement: A promising adsorbent for the removal of fluoride from aqueous solution," *J. Hazard. Mater.* 154(1-3), 88-95. DOI: 10.1016/j.jhazmat.2007.09.111
- Kim, S. J., Jung, S. H., and Kim, J. S. (2010). "Fast pyrolysis of palm kernel shells: Influence of operation parameters on the bio-oil yield and the yield of phenol and

- phenolic compounds,” *Bioresour. Technol.* 101(23), 9294-9300. DOI: 10.1016/j.biortech.2010.06.110
- Koay, Y. S., Ahamad, I. S., Nourouzi, M. M., Abdullah, L. C., and Choong, T. S. Y. (2013). “Development of novel low-cost quaternized adsorbent from palm oil agriculture waste for reactive dye removal,” *BioResources* 9(1), 66-85. DOI: 10.15376/biores.9.1.66-85
- Kumar, N. P., Kumar, N. S., and Krishnaiah, A. (2012). “Defluoridation of water using Tamarind (*Tamarindus indica*) fruit cover: Kinetics and equilibrium studies,” *J. Chil. Chem. Soc.* 57(3), 1224-1231. DOI: 10.4067/S0717-97072012000300006
- Lagergren, S. (1898). “About the theory of so-called adsorption of soluble substances,” *K. Svenska Vetenskapsakad. Handl.* 24(4), 1-39.
- Langmuir, I. (1916). “The constitution and fundamental properties of solids and liquids. Part I. Solids,” *J. Am. Chem. Soc.* 38(2), 2221-2295. DOI: 10.1021/ja02268a002
- Liu, R. X., Guo, J. L., and Tang, H. X. (2002). “Adsorption of fluoride, phosphate, and arsenate ions on a new type of ion exchange fiber,” *J. Colloid Interf. Sci.* 248(2), 268-274. DOI: 10.1006/jcis.2002.8260
- Loganathan, P., Vigneswaran, S., Kandasamy, J., and Naidu, R. (2013). “Defluoridation of drinking water using adsorption processes,” *J. Hazard. Mater.* 248, 1-19. DOI: 10.1016/j.jhazmat.2012.12.043
- Lounici, H., Addour, L., Belhocine, D., Grib, H., Nicolas, S., Bariou, B., and Mameri, N. (1997). “Study of a new technique for fluoride removal from water,” *Desalination* 114(3), 241-251. DOI: 10.1016/S0011-9164(98)00016-2
- Low, K. S., and Lee, C. K. (1997). “Quaternized rice husk as sorbent for reactive dyes,” *Bioresour. Technol.* 61(2), 121-125. DOI: 10.1016/S0960-8524(97)00054-0
- Malakootian, M., Moosazadeh, M., Yousefi, N., and Fatehizadeh, A. (2011). “Fluoride removal from aqueous solution by pumice: Case study on Kuhbonam water,” *Afr. J. Environ. Sci. Technol.* 5(4), 299-306. DOI: 10.5897/AJEST10.308
- Marshall, W. E., and Wartelle, L. H. (2004). “An anion exchange resin from soybean hulls,” *J. Chem. Technol. Biotechnol.* 79(11), 1286-1292. DOI:10.1002/jctb.1126
- Mohammad, N. S., Sivasankar, V., Mansur, Z., and Senthil, K. M. (2013). “Surface modification of pumice enhancing its fluoride adsorption capacity: An insight into kinetic and thermodynamic studies,” *Chem. Eng. J.* 228, 192-204. DOI: 10.1016/j.cej.2013.04.089
- Mohan, D., Kumar, S., and Srivastava, A. (2014). “Fluoride removal from ground water using magnetic and nonmagnetic corn stover biochars,” *Ecological Engineering* 73, 798-808. DOI: 10.1016/j.ecoleng.2014.08.017
- Mondal, N., Bhaumik, R., Baur, T., Das, B., Roy, P., and Datta, J. (2012). “Studies on defluoridation of water by tea ash: An unconventional biosorbent,” *Chem Sci Trans.* 1(2), 239-256. DOI:10.7598/cst2012.134
- MPOB (2012a). Oil Palm Planted Areas by Category as at June 2012, (http://bepi.mpob.gov.my/images/area/2012/Area_category.pdf)
- MPOB (2012b). Oil Palm Production and Stock, (http://www.mpoc.org.my/monthly_sub_page.aspx?id=435a0389-5300-4264-8e5f-e023ce9d8780).
- Namasivayam, C., and Holl, W. H. (2005). “Quaternized biomass as an anion exchanger for the removal of nitrate and other anions from water,” *J. Chem. Technol. Biotechnol.* 80(2), 164-168. DOI: 10.1002/jctb.1171

- Ng, W. P. Q., Lam, H. L., Ng, F. Y., Kamal, M., and Lim, J. H. E. (2012). "Waste-to-wealth: Green potential from palm biomass in Malaysia," *J. Clean. Prod.* 34, 57-65. DOI: 10.1016/j.jclepro.2012.04.004
- Nur, T., Loganathan, P., Nguyen, T. C., Vigneswaran, S., Singh, G., and Kandasamy, J. (2014). "Batch and column adsorption and desorption of fluoride using hydrous ferric oxide: Solution chemistry and modeling," *Chem. Eng. J.* 247(1), 93-102. DOI: 10.1016/j.cej.2014.03.009
- Orlando, U. S., Baes, A. U., Nishijima, W., and Okada, M. (2002). "A new procedure to produce lignocellulosic anion exchangers from agricultural waste materials," *Bioresour. Technol.* 83(3), 195-198. DOI: 10.1016/S0960-8524(01)00220-6
- Ornek, A., Ozacar, M., and Sengil, I. A. (2007). "Adsorption of lead onto formaldehyde or sulphuric acid treated acorn waste: Equilibrium and kinetic studies," *Biochem. Eng. J.* 37(2), 192-200. DOI: 10.1016/j.bej.2007.04.011
- Ozacar, M., and Sengil, I. A. (2005). "A kinetic study of metal complex dye sorption onto pine sawdust," *Process Biochem.* 40(2), 565-572. DOI: 10.1016/j.procbio.2004.01.032
- Parlikar, A. and Mokashi, S. (2013). "Defluoridation of water by *Moringa oleifera* – A natural adsorbent", *International Journal of Engineering Science and Innovative Technology.* 2(5), 245-252
- Pavia, D. V., Lampman, G. M., Kriz, G. S., and Vyvyan, J. R. (2009). "Introduction to spectroscopy", Fourth Edition. United State of America: BROOKS COLE Publishing Company.
- Perez, S., and Samain, D. (2010). "Structure and engineering of celluloses," *Adv. Carbohydr. Chem. Biochem.* 64, 25-116. DOI: 10.1016/S0065-2318(10)64003-6
- Ramanaiah, S., Venkata Mohan, S., and Sarma, P. (2007). "Adsorptive removal of fluoride from aqueous phase using waste fungus (*Pleurotus ostreatus* 1804) biosorbent: Kinetics evaluation," *Ecological Engineering.* 31(1), 47-56. DOI: 10.1016/j.ecoleng.2007.05.006
- Redlich, O., and Peterson, D. L. (1959). "A useful adsorption isotherm," *J. Chem. Phys.* 63(6), 1024-1026. DOI: 10.1021/j150576a611
- Riahi, K., Thayer, B. B., Mammou, A. B., Ammar, A. B., and Jaafoura, M. H. (2009). "Biosorption characteristics of phosphates from aqueous solution onto *Phoenix dactylifera* L. date palm fibers," *J. Hazard. Mater.* 170(2-3), 511-519. DOI: 10.1016/j.jhazmat.2009.05.004
- Rudzinski, W., and Panczyk, T. (2000). "Kinetics of isothermal adsorption on energetically heterogeneous solid surfaces: A new theoretical description based on the statistical rate theory of interfacial transport," *J. Chem. Phys.* 104(39), 9149-9162. DOI: 10.1021/jp000045m
- Sag, Y., and Aktay, Y. (2002). "Kinetic studies on sorption of Cr(VI) and Cu(II) ions by chitin, chitosan and *Rhizopus arrhizus*," *Biochem. Eng. J.* 12(2), 143-153. DOI: 10.1016/S1369-703X(02)00068-2
- Sips, R. (1948). "Combined form of Langmuir and Freundlich equations," *J. Chem. Phys.* 16, 490-495.
- Srimurali, M., Pragathi, A., and Karthikeyan, J. (1998). "A study on removal of fluorides from drinking water by adsorption onto low-cost materials," *Environ. Poll.* 99(2), 285-289. DOI: 10.1016/S0269-7491(97)00129-2

- Srivastav, A. L., Prabat, K. S., Srivastava, V., and Sharma, Y. C. (2013). "Application of a new adsorbents for fluoride removal aqueous solution," *J. Hazard. Mater.* 263(2), 342-352. DOI: 10.1016/j.jhazmat.2013.04.017
- Tor, A., Danaoglu, N., Arslan, G., and Cengeloglu, Y. (2009). "Removal of fluoride from water by using granular red mud: batch and column studies," *J. Hazard. Mater.* 164(1), 271-278. DOI: 10.1016/j.jhazmat.2008.08.011
- Vardhan, C. and Karthikeyan, J. (2011). "Removal of fluoride from water using low-cost materials," Fifteenth International Water Technology Conference, IWTC-15.
- Wang, L., and Li, J. (2013). "Adsorption of C.I. Reactive Red 228 dye from aqueous solution by modified cellulose from flax shive: Kinetics, equilibrium, and thermodynamics," *Ind. Crop. Prod.* 42(1), 153-158. DOI: 10.1016/j.indcrop.2012.05.031
- Wang, Y., and Reardon, E. J. (2001). "Activation and regeneration of a soil sorbent for defluoridation of drinking water," *Appl. Geochem.* 16(5), 531-539. DOI: 10.1016/S0883-2927(00)00050-0
- Wartelle, L. H., and Marshall, W. E. (2006). "Quaternized agricultural by-products as anion exchange resins," *J. Environ. Manage.* 78(2), 157-162. DOI: 10.1016/j.jenvman.2004.12.008
- Weber, W., and Morris, J. (1963). "Kinetics of adsorption on carbon from solution," *J. Sanitary Eng. Div. ASCE* 89(2), 31-60.
- WHO (1984). "Guidelines for drinking water quality," in: *Health Criteria and Other Supporting Information*, World Health Organization, Geneva, Switzerland.
- Xu, X., Gao, B. Y., Yue, Q. Y., and Zhong, Q. Q. (2010). "Preparation and utilization of wheat straw bearing amine groups for the sorption of acid and reactive dyes from aqueous solutions," *J. Hazard. Mater.* 182(1-3), 1-9. DOI: 10.1016/j.jhazmat.2010.03.071
- Yadav, A. K., Abbassi, R., Gupta, A., and Dadashzadeh, M. (2013). "Removal of fluoride from aqueous solution and groundwater by wheat straw, sawdust and activated bagasse carbon of sugarcane," *Ecological engineering* 52, 211-218. DOI: 10.1016/j.ecoleng.2012.12.069
- Yusoff, S. (2006). "Renewable energy from palm oil - Innovation on effective utilization of waste," *J. Clean. Prod.* 14(1), 87-93. DOI: 10.1016/j.jclepro.2004.07.005
- Zeldowitsch, J. (1934) "Uber den mechanismus der katalytischen oxydation von CO an MnO₂," *Acta Physicochem. URSS* 1(2), 364-449.

Article submitted: October 26, 2015; Peer review completed: November 22, 2015; Revised version received: March 7, 2016; Accepted: March 19, 2016; Published: April 4, 2016.
DOI: 10.15376/biores.11.2.4485-4511